Biophysical Chemistry 15 (1982) 245–262
Elsevier Biomedical Press

THE SODIUM CURRENTS OF NERVE UNDER VOLTAGE CLAMP AS HETEROGENEOUS KINETICS

A MODEL THAT IS CONSISTENT WITH POSSIBLE KINETIC BEHAVIOR

Kenneth A. RUBINSON *

University Chemical Laboratory, Lensfield Road, Cambridge CB2 1EW, U.K.

Received 12th August 1981

Key words: Voltage clamp; Na^+ current; Dielectric relaxation; Charge mobility; Intramembrane diffusion

A model is presented which explains the Na^+ currents of voltage-clamped nerve as resulting from a heterogeneous initiation of a sequential kinetic process. This is in analogy with the heterogeneity of the kinetics of other dielectric relaxations. The results suggest that: (1) The kinetic processes responsible for the voltage response occur within the membrane rather than at the surface; (2) The heterogeneity is due to simultaneous thermal diffusion and electric field-induced charge migration; (3) The slow turnoff upon prolonged depolarization is a voltage-independent, thermally controlled process; (4) The fast turnoff upon instantaneous repolarization is the reverse of the turning-on process. All the kinetic parameters depend on the transmembrane potential in accord with the possible behavior expected from activated-state theory. The diffusion coefficient of the charged species in the membrane as found from the data agrees with that found by photobleaching experiments on general proteins in membranes. The charge on the molecule responsible for the heterogeneous 'gating' can be calculated unambiguously from the data.

1. Introduction

Experiments using voltage-clamp techniques were successfully used to elucidate the nature of the ionic currents of axonal nerve conduction [1–4]. A consensus exists on explaining the impulse propagation using mathematical descriptions of the passive electrical response of the axon and the voltage- and time-dependent ionic permeability [5–7]. However, the mechanism causing the transmembrane ionic conduction response has been controversial since the origin of the question. A consensus exists that the channels traverse the membrane, that they are proteins, and that the electric field dependence of opening and closing must arise from the motion of charged parts of the molecule. A large number of molecular (and supramolecular) models have been constructed. A cross-section of these have been reviewed by Roy [8]. Most of those of which the author is aware utilize a concerted molecular mechanism and assume detailed voltage-dependent properties.

The detail of these algorithms is remarkable in light of the results found in the associated field of dielectric relaxation kinetics in physical chemistry. In the latter, mechanistic descriptions are, only with difficulty, extracted from far 'simpler' systems which usually can be varied over far wider ranges of pH, temperature, concentration, and solvent than a living nerve. In addition, the description of the experimental results can generally only be done by involving a distribution of relaxation times [9,10]. This is true even for small molecules in low-viscosity solvents. The larger the solute molecules and the more viscous the solvent,

* Present address: Department of Chemistry, University of Cincinnati, Cincinnati, OH 45221, U.S.A.

0301-4622/82/0000–0000/$02.75

the larger the heterogenity in the dielectric relaxation processes. The first paper in this series [11] introduced equations which account explicitly for the heterogeneous nature of dielectric relaxation as it could apply to the currents in nerve.

Chemical kinetics can be divided into three separate aspects: phenomenological laws, empirical models and theoretical mechanisms. In general, the chronology of describing the kinetics of a given system follows the trichotomy in the order given above. The phenomenological laws are the background against which the kinetics must be tested. These involve the existence of rate constants and their dependence on temperature, pressure, electric potential and chemical changes. The basis of these laws of kinetics lies in the change in energy of a chemical system and the exchange of energy and mass between its component parts as the system proceeds to its (new) equilibrium. The fundamental understanding of a system, then, lies in understanding its chemical energy which is only reflected in the rate constants. If a postulated empirical model is correct in detail, its rate constants will follow the behavior expected from the energy terms. The changes in energies for kinetics in an electric field and the possible behavior of the rate constants of elementary reactions which follow from that were described in the second paper of this series [12].

As delineated, the types of behavior of elementary kinetic processes in electric fields fall into three catagories: those associated with dipoles completely contained inside a voltage gradient; those associated with dipoles, one 'end' of which is outside the gradient (e.g., at impenetrable surfaces); and those associated with a solution of individual monopoles. We will see below that after accounting for the heterogeneity in the Na^+ voltage-clamp relaxations, the kinetics of the rise and fall of the current can be seen to be caused by processes of the latter two types and not the first. Thus, by considering the phenomenological laws and the empirical model without assumptions as to molecular mechanisms, we will find that strong suggestions of the locations and general mechanisms can, in fact, be made. The conclusions agree with the results found in recent single-channel measurements.

For the Na^+ current in a voltage-clamped nerve axon, the most significant kinetic behavior to be understood is that upon depolarization the current rise exhibits a sigmoidal form. This contrasts with the simple exponential decay (but see ref. 3) observed upon prolonged depolarization or instantaneous repolarization. Hodgkin and Huxley (the H-H model) [4] explained the kinetics in the following way. They assumed that the changes in Na^+ permeability are due to localized channels with maximum conductance being $\bar{g}_{Na}$, and that the opening and closing of each channel are governed by the movement of charged particles within the membrane. The voltage dependence of the kinetics requires that charged molecules or ions be involved. In order to fit the observed kinetics, Hodgkin and Huxley [4] suggested that the Na^+ current arises from an interaction with three of the charged particles and is then described by the kinetic function $[m(t, V)]^3$. The rapid exponential decay in response to repolarization results from the removal of a single particle. Here V is the transmembrane potential. The voltage dependence of 'm' is described by forward and reverse voltage-dependent rates $\alpha_m(V)$ and $\beta_m(V)$, respectively. In addition, the (apparently voltage-dependent) inactivation in response to prolonged depolarization is said to be caused by a separate 'blocking' particle, the action of which is described by a separate function exponential in time, $h(t, V)$, where 'h' is again described by competing rate constants $\alpha_h(V)$ and $\beta_h(V)$. Thus, the entire kinetics of the Na^+ current occurring upon depolarization and any early repolarization are described in the H-H model by $I(t, V) = g'_{Na}[m(t, V)]^3 \times h(t, V)(V - V_{Na})$.

2. The empirical model

In the following a model is described which fits the Na^+ current voltage-clamp data at least as well as the H-H model and within the experimental errors. Note that no assumptions are made concerning the voltage dependences of the parameters selected—these being ascertained from least-squares fitting of the data corrected for membrane capacitance and leakage [14] and the resistivity

difference between light and heavy waters [15]. ^2H_2O was used as a simple, reversible chemical change that might yield some insight into the molecular processes involved.

The test of the model is that the rate constants of the reactions each follow one of the possible dependencies on potential. In fact, the model yields a far more detailed picture which is consistent with the descriptive chemistry of membranes. A diffusion coefficient is found which agrees well with that measured by fluorescence diffusion for general proteins in bilayer membranes.

2.1. Assumptions

The model is formulated using kinetics based on the following assumptions.

(1) The total number of channels (the sum of both closed and open) remains constant.

(2) Individual Na^+ channels fluctuate between open and closed with the total number in each state depending on some controlling mechanism. (Channels are sites with a relatively low-potential barrier for Na^+ to cross the membrane.)

(3) The controlling process is microscopically heterogeneous.

(4) The controlling mechanism inactivates in sequence after turning on—not independently as in the H-H model.

Arguments for including heterogenity in the model follow from many sources [9,10,16–18]. In this section we discuss the mathematical model, data reduction and computer-fitting procedures.

2.2. The mathematical equations

We note that the only experimental observation is the current that passes through the set of conduction channels affected by the voltage clamp. The model is a way to dissect out individual chemical phenomena contributing to the whole effect. We thus write out the channel 'concentrations'—and infer the physical mechanisms from the rate constants' behavior found from current-curve fitting. In the following steps, the equations are derived from the four assumptions made above.

The model is formulated mathematically beginning with the kinetic expression for C in the expression

$$A \overset{k_1}{\rightarrow} C \overset{k_2}{\rightarrow} D \tag{1}$$

where A is the concentration of channels in the resting state at the depolarized potential (units = channels/unit area), C the corresponding concentration in the conducting state, and D the concentration in the closed state at the later time. We assume k_1 and k_2 are first-order rate constants. The reverse rate constant, k_{-1}, will be discussed later.

Since the only observable quantity in clamp experiments is the ion current flow, we can observe only the number of open, 'C' states. Inherent in this statement is assumption 2, that state C is either fully open or fully closed to ions with no other intermediate conducting state (but vide infra). Also, each of the channels opens over a time which is short compared to the total time of the current flow which is milliseconds.

We write initially the well known equation for the concentration at any time, t, for C in eq. 1

$$C(t) = \frac{k_1}{k_2 - k_1} a_o (e^{-k_1 t} - e^{-k_2 t}) \tag{2}$$

where, a_o is the total concentration of sites both active and passive, since we assume a conservation of channels, $A + C + D = a_o$. The time-dependent value of $C(t)$ for one set, k_1, k_2, is shown in fig. 1.

Eq. 2 is given a distribution in time using a normalized Gaussian lineshape. This function is used basically for convenience because the mathematical operation of convolution with it (explained following) is relatively easy. The mathematical form used is

$$\rho(t) = (\sigma\sqrt{2\pi})^{-1} \exp -(t - \Delta t)^2 / 2\sigma^2; \quad (t < 0) = 0 \tag{3}$$

where σ is the standard deviation and Δt the peak position in time; both are functions of potential. The Gaussian function as well as the parameters σ and Δt are illustrated in fig. 1.

Mathematically, the two functions, $C(t)$ and $\rho(t)$, can be multiplied point-by-point utilizing the formalism of convolution. This is illustrated in fig. 1 for eqs. 2 and 3. The convoluted resultant represents the fraction of total channels open over time.

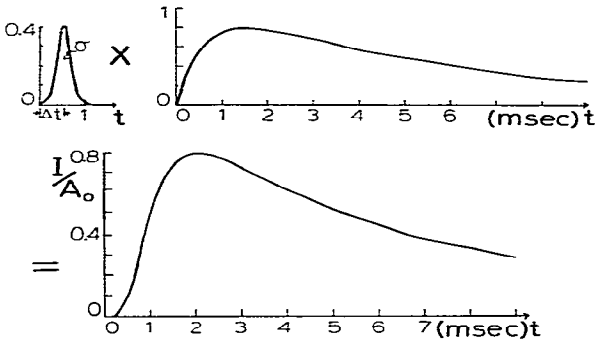

Fig. 1. Diagrammatic representation of the mathematical convolution as used for the model. Upper left is the normalized (area = 1) Gaussian distribution with its center at time Δt after the step potential jump and with a width characterized by σ. This multiplies the curve representing the reaction of channels in the conducting state, C, illustrated in the upper right. At most, about 80% are conducting at one time. The resulting curve illustrates I/A_o, the quotient of the observed current and the 'current factor'. Again, at most about 80% of the channels are conducting at one time. The values of the parameters are those determined from the current observed at 80 mV depolarization (to −20 mV absolute) from Kimura's squid nerve data.

In order to obtain a resulting current, the fraction-of-channels function is multiplied by a 'current factor', A_o. This scaling factor serves the same purpose as $\bar{g}'_{Na}$ in the Hodgkin-Huxley formalism. Here, it is first fitted empirically with no assumptions regarding its form. However, the value of A_o will depend on a number of factors. We can then write an equation including the expected factors, some of which can be separately determined. (See section 3.7.)

$$A_o = a_o \cdot \mu_{Na} \cdot f \cdot g_{Na} \cdot \text{area}. \tag{4}$$

These factors are, respectively: a_o, the total number of channels per cm^2; μ_{Na}, the electrochemical driving force; f, the measure of the fraction of channels activated; g_{Na} the conductance of Na^+ inside the voltage clamp; and the area in cm^2.

The inclusion of f results from the expectation that not all the a_o channels may be activated or activatable at all depolarization potentials: only some fraction between 0 and 1 of the total, a_o. The conductance factor, g_{Na}, includes the uncompensated series resistance and the 'open'-channel resistance, the latter of which may be voltage dependent. The electrochemical potential function, μ_{Na}, itself depends on the Na^+ equilibrium (Nernstian) potential, V_{Na}, and the transmembrane potential, V. We make no assumptions about the descriptive mathematical form of the electrochemical potentials, since any detailed description involves assumptions for which there is no independent experimental basis. One likely complication, for instance, involves having an effectively electrically asymmetric membrane. As will be seen, the resulting A_o values as a function of transmembrane potential allow the effects of the electrochemical potential to be separated in a reasonable way.

The total, time-dependent part of the current then is written (see the full derivation in the Appendix)

$$I(t) = (2\pi\sigma^2)^{-1/2}[k_1/(k_2-k_1)] \cdot A_o \cdot \int_{-\infty}^{t-\Delta t} \{\exp[-k_1(t-u-\Delta t)] - \exp[-k_2(t-u-\Delta t)]\} \cdot \exp[-u^2/2\sigma^2]\, du \tag{5}$$

Here u is a false variable of integration and has no physical meaning. The parameters Δt and σ are defined in fig. 1 and eq. 3. The form of eq. 5 used for the computer is shown in the Appendix.

2.3. Experiments and computations

Na^+ current data were obtained personally from Drs. J. Kimura, C. Schauf and H. Meves. The appropriate figure captions acknowledge their contributions specifically.

For the ^2H_2O-bathed nerve, a correction to the measured current was made to account for the lower conductivity of ^2H_2O relative to H_2O. This changes the current as measured across the double C electrode. The value of the correction is 1.22 [19]. Thus, the A_o terms of the H_2O and ^2H_2O experiments can be compared directly.

Computer fitting of the data was done by a least-squares routine using programs in the NAG Library of the Cambridge University Computer Centre. The independent variables of the nonlinear equation could include all five, A_o, Δt, σ, k_1 and k_2. Alternatively, any number of these could

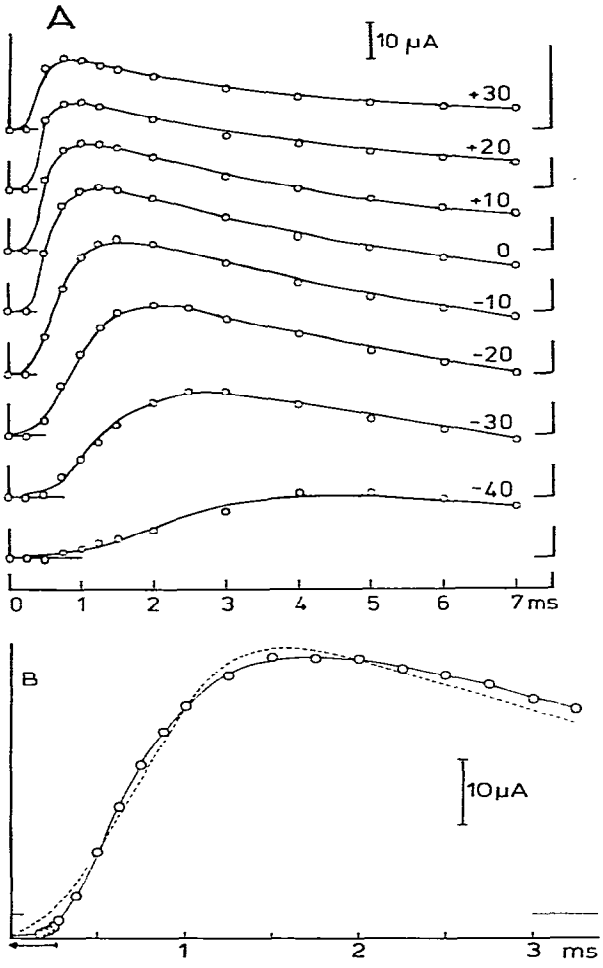

Fig. 2. (A) The Na^+ currents for squid at 1.5°C. Data courtesy of Dr. J. Kimura. The holding potential was −100 mV with a step depolarization to the voltage shown over each curve. Circles are data points, the lines are the least-squares fits to the data. (B) A comparison of the least-squares fits using the Hodgkin-Huxley equations (-------) and the model presented here (————). This is the initial part of the 60 mV depolarization of Meves data in H_2O. The horizontal line segments above the baseline shown mark the 'baseline' after all corrections have been made; i.e., a small uncorrectable outward current sums with the inward Na^+ current at least in the initial region. Because of the uncertainty of the time course of the outward current, and the relative size of known corrections, the data points at less than 0.25 ms (small arrow at left) are far less certain. the parameter values used to fit the data are, using the Hodgkin-Huxley equations, $\tau_m = 0.578$ ms, $\tau_h = 3.877$ ms, $\bar{g}_{Na}$ = 27.3 mmho cm^{-2}) which is equivalent to a 'current term' in the present model of 80.5 μA. For the statistical triggering model, the parameter values are $k_1 = 1623\ s^{-1}$, $k_2 = 232\ s^{-1}$, $\sigma = 142$ μs, $\Delta t = 345$ μs, and the current term is 60.4 μA.

be held constant at a fixed value. In general, the least-squares fitting was so facile that at least one variable could be held constant with little change in the residual values which indicated excellence of fit.

2.4. Sensitivity of parameter fit

The most reproducible and most sensitive variable is the overall scaling factor, A_0, since it affects the error of all points. It was even independent of the normalized kinetic model (others have been made by the author). A typical fit to the data is shown in fig. 2. It is estimated that the limitations to the fits is the accuracy of the data reduction. The calculated variable values were relatively insensitive to the corrections made for currents due to membrane leakage and polarization. The effects of differences in the tail were reflected mostly in k_2. This is, next to A_0, the most sensitive variable. As might be expected, σ, Δt and k_1 interact to various degrees. The extent of empirical separability of the $(\sigma, \Delta t)$-process from that described by k_1 can be argued as follows. A simple measure of the termination of the triggering process is $(\Delta t + 2\sigma)$. More than 95% of the channels will have fired by then. These times are about the same point as the inflection of the rise of the current flows. Usually, a relatively long time elapses from then until the peak and subsequent decay of the current. Thus, the variables $(\Delta t, \sigma)$ and k_1 are determined in the curve fitting, each primarily by a different part of the current response in general. At higher temperatures, however, the separability of σ and Δt from k_1 is less clear and scatter in their behavior (especially k_1 and σ) results.

It may be noted in passing that in using the system $A \xrightarrow{k_0} B \xrightarrow{k_1} C \xrightarrow{k_2} D$, where C is conducting, the least-squares fits to the data are inferior to the model described here. This is especially true for the nerves in ^2H_2O.

3. Results

3.1. The values of Δt

The time at the peak of the distribution of triggering times, as found from the least-squares fit, is called Δt. This is illustrated in fig. 1. Its values are shown in table 1.

Empirically, a plot of $1/\Delta t$ versus ΔV, the potential step size, is found to be linear. This is shown in fig. 3. This behavior, being linear with potential jump over a range of values of about a factor of four, is the type expected for movement of charges in ionic conduction [12].

For the process of ionic conduction, we expect the ion velocities to be directly proportional to the effective field with the flow becoming infinitely slow when the potential change is zero. Thus, the intercept with the voltage axis, $(1/\Delta t) = 0$, will indicate the true, effective zero of the potential jump. This differs from the applied potential jump by a constant value for each nerve. (See fig. 3.)

Table 2 shows the holding potential and apparent zero potentials (voltage-axis intercept) as experienced by the charged species involved in the 'Δt-process.' The correction between the applied

Table 1

Parameter values from computer least-squares fit

Depolarization (mV)	k_1 ($k_2 = 220$) (ms^{-1})	k_2 (ms^{-1})	Δt (μs)	σ (μs)	A_o; $k_2 = 220$ (μA)
Meves: H_2O					
30	613 (1716)	324	1450	1195	11.44
40	1188 (1419)	242	541	355	30.4
50	2255 (2249)	219	414	285	41.8
60*	2650 (1705)	232	349	142	56.8
70	2500 (2606)	231	286	91	49.2
80	3204 (3457)	234	239	57	37.2
Depolarization (mV)	**k_1 ($k_2 = 160$) (ms^{-1})**	**k_2 (ms^{-1})**	**Δt (μs)**	**σ (μs)**	**A_o; $k_2 = 160$ (μA)**
Meves: ^2H_2O					
40	487 (549)	175	1203	601	40.5
50	1226 (1230)	160	864	452	41.8
60	1266 (1167)	152	519	177	56.8
70	1619 (1756)	183	439	177	49.3
80	2866 (2860)	153	372	157	40.6
90	3374 (3537)	181	316	105	31.7
100	4250 (5199)	197	280	88	22.9
110	4213 (5233)	198	248	90	16.7
Depolarization (mV)	**k_1 ($k_2 = 180$) (ms^{-1})**	**k_2 (ms^{-1})**	**Δt (μs)**	**σ (μs)**	**A_o; $k_2 = 180$ (μA)**
Kimura: H_2O					
60	301 (504)	297	1097	407	29.6
70	974 (996)	186	685	195	39.8
80	1795 (1578)	164	542	147	45.3
90	2412 (2332)	176	398	73	43.7
100	3540 (3700)	184	349	36	38.4
110	4854 (5559)	191	314	31	32.2
120	7233 (9526)	199	319	27	25.3
130	(>10000)	199	246	7	21.6

Table 2

Corrected voltages for clamp potential jumps

Nerve/expt.	Holding potential (mV)	Depolarization correction (mV)	Corrected 'first current' depolarization (mV)
Kimura/squid	−100	41	19±5
Meves			
squid/H_2O	−80	6	24
squid/^2H_2O	−78	21	19
Schauf/*Myxicola*	−100	46	14

and apparent zero is shown in the third column of the table, and the new, corrected zero is seen in the fourth column. The first analyzable pulse in the voltage clamp is seen at the potential displayed in the last column. This is when a current response has a peak in the time period monitored. It appears that the 'triggering' process is consistent; it is effective above about 20 mV corrected depolarization jump and independent of the steady holding potential.

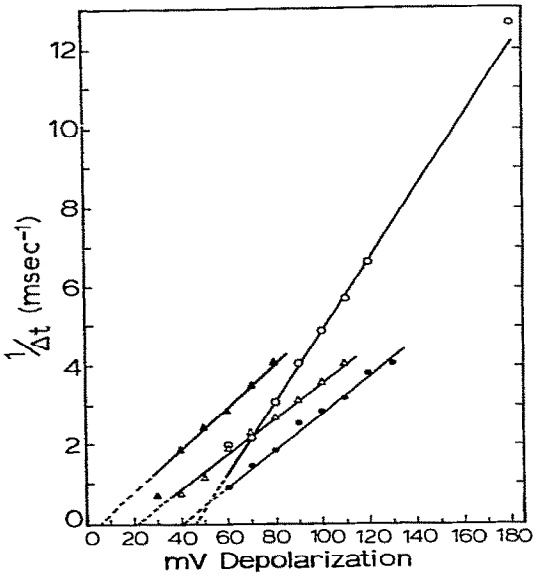

Fig. 3. Plot of $(\Delta t)^{-1}$, found from least-squares fits, versus the potential step size for the following data. ▲, Meves H_2O data for squid; △, the same nerve with ^2H_2O; O, *Myxicola* data; ●, Kimura's squid data. The conditions of measurement are listed in table 3. An unconstrained least-squares fitting routine was used, i.e., no parameters were held constant. The lines were fitted by eye.

One possible reason for the difference between the applied voltage pulse and the effective jump could be a changing interface potential. This might be expected to be roughly proportional to the holding potential and to relax quickly relative to the Δt-process [20]. This interface potential results from such detailed mechanisms as reorientation of surface dipoles. Also, any other capacitance-producing mechanism of the membrane-interface system will cause such an effect. This is the first of a number of results that suggest the Δt-process occurs inside the membrane.

As a result of the linearity with voltage, the cause of the delay, Δt, is seen to arise from a diffusion process [12]. These occur in free solution in response to an electric field as in electrophoresis. Also, such processes occur across liquid/liquid interfaces when the interface is permeable to ionic species.* There is no permanent potential established due to the ions [20,21]. In other words, we would expect a potential to be established across

* The 'surface' of a liquid or solid is generally considered to be about 10 Å deep. Below that level, bulk properties are considered to ensue. Since the polar region on the lipid bilayer is only about that thick, it may be more useful to consider the membrane to be a polar oil rather than a layered polar-nonpolar-polar structure. That is, the membrane properties are an average of its conceptual sections at least in certain regions. Such a view may be helpful in further interpretation of the Δt-process.

an interface by an externally imposed voltage. But then ions would flow across the interface until the effects of the field were neutralized. While such a mechanism is suggested by the above results, the detailed location of the interface is unknown: e.g., it could be a membrane/solution or membrane/protein interface.

We now make an order-of-magnitude calculation of the charge mobility associated with Δt. From it, the ionic mobility of the charge(s) responsible for the Δt-process can be calculated within an order of magnitude. Let us assume that a fixed amount of charge is transported across the interface after the depolarization. (If this is not true, the difference will be taken up in the value of A_0.) This charge is transported an average distance, $\bar{d} = v \cdot \Delta t$, and the velocity, v, is related to the ion mobility by $v = u|z|V$. Here, u is the mobility, z the ion charge and V the potential. We have seen above that this potential is the effective potential jump, ΔV_{eff}. We now use the following relationship [22] for the force on a charge.

$$\text{Force} = 1.60 \times 10^{-12}/|z| \text{ dyne V}^{-1} \text{ cm}^{-1}.$$

Applying a pulse jump of 100 mV across the membrane, the time $\Delta t \approx 1 \times 10^{-4}$ s. We can assume an average distance of the order of 10 Å (certainly about 1–100 Å.) Thus, the velocity

$$v = 10^{-7}/10^{-4} = 10^{-3} \text{ cm s}^{-1}$$

The field is about $0.1/10^{-7} = 10^6$ V cm^{-1} ignoring any dielectric constant effects. The force is then $1.6 \times z \times 10^{-6}|z|$dyne. The ionic mobility, u, is related to the velocity by

$$u = v \cdot \text{force} = 10^{-3} \times 1.6 \times 10^{-6} = 2 \times 10^{-9}|z| \text{ cm s}^{-1} \text{ dyne}^{-1}$$

For $z = 0.1$–10, this is of the order of values found for ions in ionic solids and for metals in liquid metals [23]. Even allowing for the largest possible dielectric effects, the value again suggests that the ion motion associated with the Δt-process occurs inside the membrane.

Checking the effectiveness of this simple order-of-magnitude calculation, if the charged entity were an Na^+, from the Stokes' formula [22], the viscosity is suggested to be about 10^{+5} P. If the charged species were in water, with viscosity 1 cP, its radius would be absurd: 3.3×10^{17} Å when the charge is 1.

In conclusion, the Δt-process appears to arise from an ion-conduction mechanism which occurs inside the membrane. The conclusion is based on (1) the linear dependence of $(1/\Delta t)$ with ΔV, (2) the existence of an apparent surface capacitance polarization which changes the applied potential jump as experienced by the charges responsible for the Δt-process, and (3) a rough calculation of apparent viscosity which shows a viscosity expected for a solid or highly viscous liquid.

3.2. The values of σ

The triggering and its distribution are a result of the motion of some charged species, since the variable, Δt, characterizing its peak position is voltage dependent. We have envisioned this process to be a sheet of charge moving some distance in order to redistribute the charge to conform to a new equilibrium in the changed external field (see fig. 4). The value of Δt (in time units) is thus related through a velocity to the motional distance (in spatial units).

Concurrently, the width of the distribution as characterized by the variable σ, the standard deviation of the Gaussian, changes as well. From simple symmetry arguments, it can be seen that the externally applied, directional field cannot broaden or narrow the width of a charge distribution simultaneously in both the forward and following directions. In other words, Δt, measuring the peak position in time, must express the entire voltage dependence of the motion of a plane of charge. It follows that the width, σ, will be independent of voltage. The process characterized by σ will then be diffusional. It is allowed to proceed for a time Δt; material will diffuse further during longer Δt values than shorter ones. The argument for the dependence of σ on Δt follows. The derivation involves transforming from the spatial ion distribution to the temporal distribution derived from the measured Na^+ currents.

This derivation is shown pictorially in fig. 4. Here is displayed the cross-section of the charge density of the sheet of charge of the Δt-process in space. It is shown as it has evolved at different times as the plane of charge proceeds across the average distance $\bar{d}$. Let us call σ in the space-

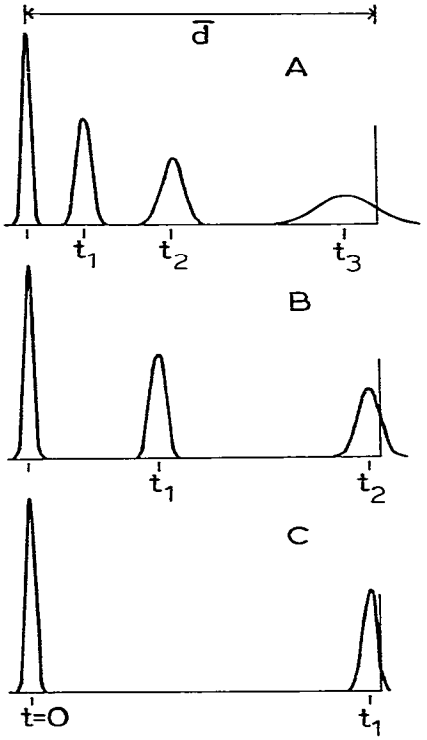

Fig. 4. Diagrammatic plot of the Gaussian cross-section of differential charge density as it varies with time and potential. The triggering effect occurs when the charges reach the line at the right, a distance $\bar{d}$ away from the original position. $t_1 < t_2 < t_3$. The center of charge sits at the position at the left at the holding potential. At $t = 0$ it begins to move. In case A (top), the potential jump is small and the time taken to traverse the distance $\bar{d}$ is long (t_3). In that time, diffusion of the charges takes place to form a relatively broad band of charge. In case B, the potential jump is intermediate and the narrower distribution reaches the 'target' after a shorter time (t_2). In case C, the potential is large, and a narrowly distributed sheet of charge reaches the target at time t_1. The behavior illustrated here is the basis for the analysis of the relationship between σ and Δt presented in the text.

domain σ_x for the purposes of discussion. The distribution widens as time procceds. Given a value of σ_x^0 at $t = 0$, σ_x moves out from the center of the Gaussian at a rate such that $(\sigma_x - \sigma_x^0) = \sqrt{2Dt}$, a simple diffusion relation. For the present we assume $\sigma_x^0 = 0$.

In the model, we measure the 'arrival' or effect of charge at time Δt at the position given by the line at the right-hand side of fig. 4. The time course that the distribution of the spatially spreading sheet of charge follows crossing the line (i.e., having its effect on the channel) determines the value of σ obtained from the least-squares fit of the data. Call the value of σ in the time domain σ_t to distinguish it from the spatial σ_x. These two measures are related by the simple equation

$$\sigma_x = \sigma_t \cdot v = \sigma_t (\bar{d}/\Delta t) \tag{6}$$

where v is the velocity as used before in the discussion of Δt. Then, substituting the value of σ_x given in eq. 6 into the diffusion relation

$$\sqrt{2D \cdot \Delta t} = \sigma_t \cdot (\bar{d}/\Delta t) \text{ or } \sigma_t = (\sqrt{2D}/\bar{d}) \cdot \Delta t^{3/2}. \tag{7}$$

In fig. 5, we plot the values of σ versus $\Delta t^{3/2}$ for the data. (The data of σ and Δt determined from Meves' H_2O data are too scattered to use for interpretation. This is due to bad separability from k_1.) From the graphs, the slope is about 14 $s^{-1/2}$.* Therefore, $\sqrt{2D}/\bar{d} \approx 14$ $s^{-1/2}$. Using the assumed, approximate value of 10 Å for $\bar{d}$, as used in the previous section, we calculate a value of $D \approx 10^{-12}$ cm^2 s^{-1}. Note that any reasonable choice of $\bar{d}$, from 0.1 to 100 Å, yields a value for D that is typical for ionic motion in solids [23].

This value is also in agreement with data measuring lateral diffusion in erythrocyte bilayers by fluorescence redistribution [24]. In that work, the measured, average diffusion coefficient values for membrane glycoproteins was $D = 2 \times 10^{-11}$ cm^2 s^{-1} at 30°C).

Following Jost (p. 136 of ref. 23), we can use the approximation for ions in solids

$$D \approx 3 \times 10^{-4} \exp(-\Delta G/RT)$$

to obtain $\Delta G^{\ddagger} \approx 11$ kcal/mol^{-1}. The values derived from future experiments at different pH values, temperatures, solvents and ion substitutes

* The intercepts of the lines are not exactly zero. The detailed analysis of this will require further data. The cause of the intercept of the σ-axis could be an inherent width ($\sigma_x^0 \neq 0$). Alternatively, perhaps, some form of change in the relative initial charge position at the low holding potential will cause the intercept to appear with an intercept on the Δt-axis.

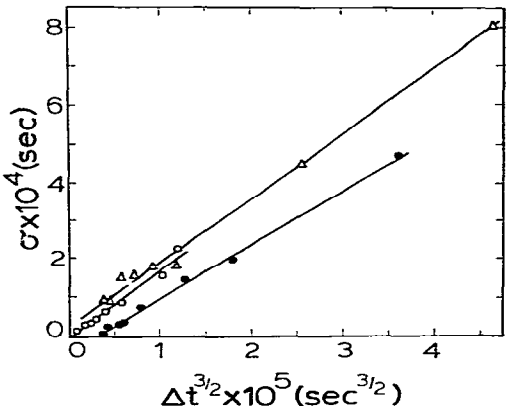

Fig. 5. A plot of the least-squares values of σ versus $\Delta t^{3/2}$ for the various nerves. (△) Meves ^2H_2O experiment, (○) from *Myxicola*, and (●) Kimura's squid data. Meves H_2O data were too scattered to have any meaning due to interference with effects in the fitting due to the k_1-process. The slopes of the lines are equal to $\sqrt{2D}/\bar{d}$. The straight lines are least-squares fits. The fitting equations are $\sigma = 16.88 \cdot \Delta t^{3/2} + 1.49 \times 10^{-5}$; $\sigma = 17.75 \cdot \Delta t^{3/2} - 0.75 \times 10^{-5}$; and $\sigma = 14.1 \cdot \Delta t^{3/2} - 4.44 \times 10^{-5}$ (top to bottom, respectively).

may be useful in characterizing the detailed process contributing to the value of σ.

However, the description of the behavior of σ and Δt alone serves to explain, at least qualitatively, the differences in the 'delay foot' of the current transients. These become longer with hyperpolarizing prepulses. The value of Δt changes linearly with the depolarization pulse. σ changes faster with an apparent dependence of $\Delta V^{3/2}$ due to its dependence on $\Delta t^{3/2}$. Thus, the distribution will tend to appear to 'sharpen' with larger depolarizations. This will then cause the current response to appear to have a longer 'foot'. The change in the foot with the length of the prepulse reflects the time required to establish the new steady-state charge distribution. These can be clarified by further careful curve fitting. Future experiments should be carried out at lower temperatures, and using ^2H_2O seems to allow better separation of k_1 from the σ and Δt variables. Such conditions will most clearly enhance the consistency of all three.

A final observation about the analysis concerns a distortion of the distribution that may show up during small depolarizations. If the velocity of the ion sheet is slow, the time taken for the distribution to arrive at the 'line' can be so long that appreciable further diffusion can occur at the trailing side while the leading side is already sensed. The distribution as measured in time will appear to be distorted with a 'tailing'. This will tend to distort the whole current curve. The curve fitting does not account for the distortion; the values of both k_1 and k_2 will be affected. This could be the cause of the apparently anomalous value of k_2 at low depolarizations. (See section 3.5.) Recently, such a distribution was found experimentally for muscle measuring single-channel triggering distributions [25].

In conclusion, the values of σ found from the least-squares fitting of the data are related linearly to $\Delta t^{3/2}$ with a slope of about 14 $s^{-1/2}$. From this value, an approximate value for D, the diffusion coefficient, can be found assuming reasonable distances of travel. The calculated diffusion coefficients are characteristic of solid-state diffusion and reinforce the conclusion that the $(\sigma, \Delta t)$-process occurs inside the membrane. *

3.3. Calculation of the charge involved in the $(\sigma, \Delta t)$-process

Ware and Flygare [26] measured the time-average values of both the diffusion coefficient and electrophoretic mobility simultaneously for serum albumin in solution. However, to the author's knowledge, no measurement has been made on any material where the effect of the time evolution of the voltage-driven ionic transport and the random thermal diffusion could be observed at the same time. Thus, the treatment of this problem is dwelt upon at some length below.

In the analysis made in the preceding section, the parameter Δt describes the voltage-dependent part of the charge transport. σ describes the voltage-independent transport: In other words, σ represents the effects of diffusion *in the moving frame of reference.* The two types of transport are separately characterized by two different parameters, and so the two classical transport equations can be

* See footnote, p. 251.

solved simultaneously and applied to the analysis.

For the electric field-induced transport, Stokes' equation can be used, i.e.,

$$v = \frac{F|z|}{6\pi\eta r} \tag{8}$$

where F has the units of force V^{-1} cm^{-1} unit charge^{-1}. η is the solution viscosity and r the radius of the charged unit.

For the purely diffusive part, the Einstein-Stokes equation applies

$$D = \frac{kT}{6\pi\eta r}. \tag{9}$$

The denominators can be set equal and we can write

$$\frac{F|z|}{v} = \frac{kT}{D}. \tag{10}$$

Numerical values can be substituted into eq. 10 and an unambiguous value of the net charge transported, $|z|$, for the $(\sigma, \Delta t)$-process can be calculated. First, as noted in eq. 7, the slope of the plot of σ versus $\Delta t^{3/2}$ is $\sqrt{2D}/\bar{d}$ (fig. 5). This relates the diffusion coefficient to the distance traveled. Experimentally, $\sqrt{2D}/\bar{d} = 14$ or $D = 114\bar{d}^2$. Second, the value of the velocity is replacing using $v = \bar{d}/\Delta t$. Third, the value of $F|z|$, the force on a charge $|z|$ in a unit electric field, is $F|z| = 1.6 \times 10^{-12}|z|$ dyne V^{-1} cm^{-1} [22]. The change in electric field in (V cm^{-1}) is related to the potential jump by $\Delta E = (\Delta V_{eff}/\bar{d})$. Together,

$$F|z| = \frac{V_{eff}}{\bar{d}} \times 1.60 \times 10^{-12}|z| \text{ dyne.}$$

Thus, eq. 10 can be rewritten

$$\frac{V_{eff}\Delta t}{\bar{d}^2} \times 1.6 \times 10^{-12}|z| = \frac{kT}{114\bar{d}^2} \tag{11}$$

Since the arbitrary value $\bar{d}$ drops out,

$$|z| = kT/(114 \cdot \Delta V_{eff} \cdot \Delta t \cdot 1.6 \times 10^{-12}) \tag{12}$$

Then we substitute $k = 1.38 \times 10^{-16}$, $T = 280$ K, and the constant value of $\Delta V_{eff} \cdot \Delta t = 2 \times 10^{-5}$ V s from Kimura's H_2O data as seen in fig. 3. Thus, eq. 12 can be solved for the value of $|z|$ unambiguously. The value of $|z| = 10.6$ elementary charges. From the plots of fig. 5, this value could be as low as 8.6. It will be interesting to see whether the value changes with pH or temperature on the same nerve in the same bathing medium.

From the value of $|z|$, the electric field energy available from the charge transport can be calculated. We consider that the threshold for a triggering of the channels occurs at about 20 mV depolarization (after correction for shielding—see table 2). With the assumption that the approx. 10 charges traverse the entire potential, the energy available is 4.6 kcal mol^{-1}. This is enough to break about two to four hydrogen bonds.

3.4. The values of k_1

After the heterogeneous triggering, the current appears with a rate characterized by a first-order rate constant, k_1. The values of k_1 are found from the computer fitting. A plot of these values is seen

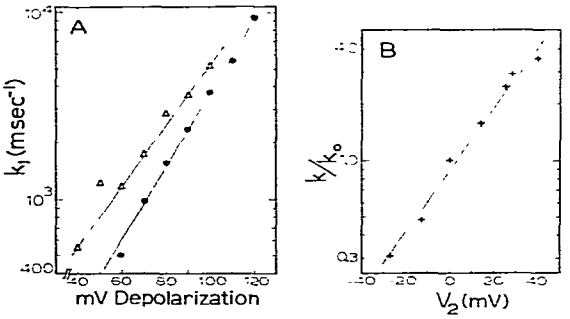

Fig. 6. (A) Plot of log k_1 versus depolarization (mV) for squid nerve. The numerical values are shown in table 1. (●) Kimura's data with $k_2 = 180$ held constant. (△) Meves ^2H_2O data with $k_2 = 160$ held constant. For a 10-fold change in rate, the slopes of the straight lines are, respectively, 54 and 61 mV. The data of Meves for the nerve in H_2O are too scattered to have significance; this scattering arises from lack of a clear separation of the k_1- and Δt-processes. (B) Data for instantaneous repolarization from Hodgkin and Huxley [3]. This is replotted from fig. 9 (p. 484) of this paper. Axon 25 was pulsed to 110 mV absolute and returned to $-V_2$. This is the process characterized by β_m. The ordinate is the ratio of the rate constant measured compared to that measured at $V_2 = 0$. Since the voltage scale in the original paper is reversed from the contemporary sense, the abscissa scale is reversed from that in A. The line drawn has slope -61 mV. The similarity of the slopes (with the reverse sign) in A and B suggest that the β_m-process is the reverse of that characterized by k_1.

in fig. 6A. They follow the behavior [12]

$$(\mathrm{d}\log k_1)/\mathrm{d}V=(\Delta z^{\ddagger}F\alpha')/RT=\text{constant} \qquad (13)$$

where $\Delta z^{\ddagger}$ is the charge of activation, F the Faraday constant, R the gas constant, and T the absolute temperature. α' is the transmission coefficient [27,28]. This behavior is characteristic for an 'interface polarization' [12].

The line fit in fig. 6A is entirely adequate without considering a simultaneous, reverse reaction characterized by k_{-1}. This simple behavior might be explained by referring to experience with simple exponential—first-order—kinetics. It is difficult to separate out two concurrent processes where the rates differ by less than about a factor of two; the sum of two exponential relaxation pathways is difficult to discern from a slightly skewed single-exponential process unless each can be measured independently. Now assume that the two concurrent reactions are in opposite directions with one rate at least 10-times faster. An example is

$$X \underset{k_{-1}}{\overset{k_1}{\rightleftharpoons}} Y: \quad k_1 > 10k_{-1}$$

where the contribution of the reverse process to the relaxation rate constant will be difficult to detect in an experiment measuring only the overall rate of relaxation due to a perturbation of the equilibrium. It follows that a complete description of all the forward and reverse rate constants may not be possible unless they happen to fall in a narrow, convenient relative range at the potential used. (See ref. 12 and references therein.)

In the case of the k_1 and k_{-1} (or the Hodgkin-Huxley β_m) rate constants, a change by a factor of 10 in the relative rates occurs over only 30 mV (vide infra): one accelerates by a factor of three and the other decelerates by the same factor. So we can consider only the forward rate process alone although both forward and reverse reactions proceed at the same time. However, due to their strong voltage dependence, the rate-determining step of the reaction arises from the charge polarization in one direction only. The progress of the reverse process is negligible.

The criterion of reversibility of interface polarization requires an approximately equal but opposite slope in eq. 13 for the forward and reverse reactions. This requirement seems to be fulfilled in the kinetic pairing of the k_1 forward process discussed here and the reverse, β_m, process (in the Hodgkin-Huxley nomenclature). These are illustrated in fig. 6A and B. In fig. 6A, the values of k_1 from the computer fitting are shown for two squid nerves. In fig. 6B, the data of fig. 9 in ref. 3 (p. 484) are replotted. The voltage scales are, in effect, reversed between fig. 6A and B, since the old nomenclature is used in the latter. This presentation shows clearly the similarity of slopes derived from the directly measured 'fast turnoff' on the nerve and the turning-on as extracted from the statistical triggering model. If the temperature dependencies of these rates are parallel, the suggestion that these processes are., indeed, the reverse of each other will be strengthened. Similarly, if both have the same hydrogen-deuterium isotope effects, the conclusion will be firmer still.

One caution is needed, however. The slopes do not have to be exactly equal for a given nerve, since α' for the forward and reverse reactions can be different according to charge-transfer theory [28].

Concerning the origin of the k_1-process, the value of the slope, $(\Delta zF\alpha')/RT$, is greater than 54 mV which is expected around 0–5°C for a monovalent charge traversing the total potential drop. Since α cannot be greater than 1, this result suggests that a lower limit to $\Delta z^{\ddagger}$ is about 1.13 charges.

Recently, single-channel measurements of Na^+ current flows have been interpreted as requiring Na^+ to fill empty binding sites within a pore for conduction to occur [29]. This hypothesis is qualitatively in agreement with the above analysis, since a surface polarization will occur at the ion-selective pores. Also, the agreement is quantitative with the charges causing the process being monovalent.

3.5. *The values of k_2*

The values of k_2 from an unconstrained least-squares fit (σ, Δt, k_1, k_2, A_o all freely varying) are displayed in table 1. The values are plotted versus depolarization voltage in fig. 7. Overall, the value of the variable appears to be independent of volt-

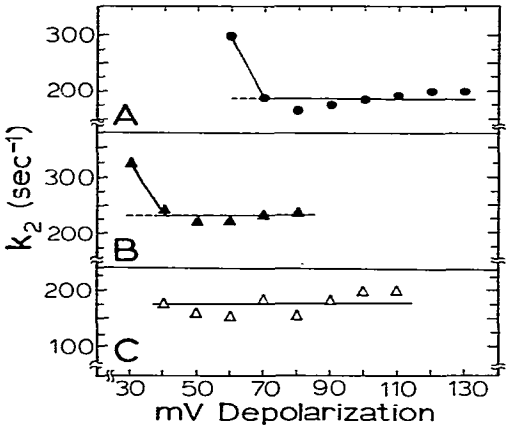

Fig. 7. Plots of the values of k_2 from the least-squares fitting of the model equation versus depolarization step potential size. (A) Kimura's data from a squid nerve in H_2O. (B) Meves' data on a nerve in H_2O. (C) the same nerve in ^2H_2O. The straight lines are at the average values.

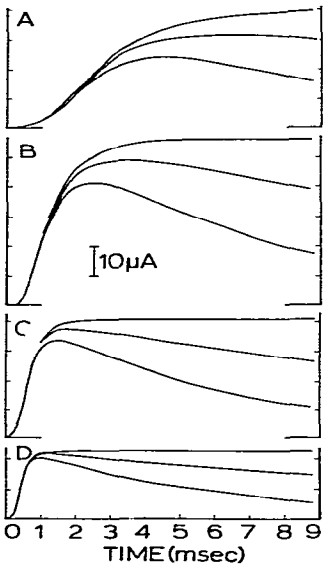

Fig. 8. Simulation of the voltage-clamp currents with changes in the value of k_2. The bottom curve of each is the least-squares fit to Meves ^2H_2O data at 40, 60, 80 and 100 mV depolarization from a holding potential of −78 mV. In each, $k_2 = 160$. The two curves above each of these are calculated using $k_2 = 50$ and 0, respectively. This simple change mimics the experimental results on a nerve treated with pronase internally. A slowing of k_2 kinetics mimics the changes seen with trinitrophenol.

age. The values for the same nerve in H_2O and ^2H_2O (fig. 7B and C) are $k_2(H_2O) = 220$ and $k_2(^2H_2O) = 160$, respectively, at 4°C. The constant value of k_2 is determined from the average of the values—excluding the anomalous one if present. As discussed above, the anomalous value of k_2 (found for the smallest analyzable depolarization current) may result from the use of an imperfect distribution function.

If the value of k_2 is independent of potential as indicated, the rate of the process must be thermally determined. The nature of the process can perhaps be clarified by referring to chemical modifications which are known to change the rate of the channel closure. Perhaps the most informative of these experiments is the addition of trinitrophenol to the bathing medium. This behavior can be mimicked quite well by using smaller values of k_2 in simulations. A sketch of such changes for a hypothetical experiment is shown in fig. 8. The chemistry of trinitrophenol is varied but it can behave as an ion trap [30], i.e., it could interfere with ion recombination. This is consistent with the voltage independence of the k_2-process.

Onsager [31] and Mozumder [32] have shown, and others have demonstrated the validity in solutions [33,34] and in the solid state [35], of the diffusion-controlled ion recombination in an electric field. The separation process is voltage dependent while recombination is not. Other possible mechanisms of action have been discussed by Oxford and Pooler [36].

If the values of k_2 are, indeed, completely voltage independent, then a simple enthalpy and entropy of activation should be able to explain the temperature dependence. The fitting of data from nerves having their k_2-process altered might yield effective equilibrium constants or dose-response curves for the binding.

3.6. Overview of the kinetic factors

Four variables are used here to fit the time-dependent part of the Na^+ currents seen in simple voltage-clamp experiments. These are σ, Δt, k_1, and k_2. The values of the parameters are simple functions of the potential jump and follow known chemical behavior.

The turnoff upon prolonged depolarization is characterized by a rate constant k_2. This is a single number: a simple, voltage-independent rate constant.

The change in values of k_1 with potential jump can be described using a single charge of activation, $\Delta z^{\ddagger}$. The functional dependence of the rate constant with voltage follows from activated-state theory.

The values of Δt for all potentials are explained using the equivalent of a single molecular mobility. A correction is required for partial shielding of the external voltage change.

The values of σ can be interpreted using a single diffusion coefficient for a species migrating for a time, Δt. The combination of the behavior of σ and Δt can be used to calculate a value of the charge of the species responsible for the process.

And finally, as required from symmetry, the same $\Delta z^{\ddagger}$ that describes the voltage-dependent change in k_1 also describes the potential dependence of the reverse process. The latter is that characterized by the β_m of Hodgkin and Huxley.

3.7. *The values of A_o*

Reproduced here is eq. 4 for the current flowing through the active channels

$$A_o = a_o \cdot \mu_{Na} \cdot f \cdot g_{Na} \cdot \text{area} \qquad (4)$$

where a_o is the number of channels/cm^2, μ_{Na} the chemical potential in the transmembrane concentration gradient, f the fraction of channels that open, g_{Na} the conductivity of a channel + (series resistance/channel)$^{-1}$ and area is the area of the sampled nerve in cm^2.

Inherent in this factoring is the assumption that there are no 'partly conducting' channels. This follows from the assumption that the number of channels, a_o, is constant and is voltage independent. Thus, the product $f \cdot a_o$ is a proper description of the number of channels that can pass through the conducting state. Since there appears to be no independent proof for these statements, this factoring must be considered provisional. For instance, if all the channels have reduced conductance at low potentials, but all are active, f would become the 'fraction of maximum conductivity' for each channel.

General agreement seems to prevail that the chemical potential defines the ionic driving force across the membrane. This is supported by multiple-pulse clamp experiments where the so-called instantaneous currents follow the relation $g_{Na}(V - V_{Na})$ where V_{Na} is the *effective* Nernstian potential. Here, in this new description, the A_o term relates the same information as the instantaneous currents measurements except that the whole current response over time is used to determine it. There is the added advantage that special multiple-pulse experiments need not be done to measure them; this is an inherent part of the analysis due to using 'channel-conserving' kinetics.

The values of A_o from the least-squares fitting are displayed in fig. 9. However, because the behavior of the values with voltage are not derived from symmetry relations as are the kinetic rate constants, some assumptions must be made to separate the values of each (or sets) of the factors in eq. 4 in order to explain the curves.

From fig. 9 we see that the values of A_o follow a linear relationship with voltage for the squid nerve from about -10 mV to the highest analyzable transmembrane potential where a kinetic analysis could be done accurately. Assuming that the entire

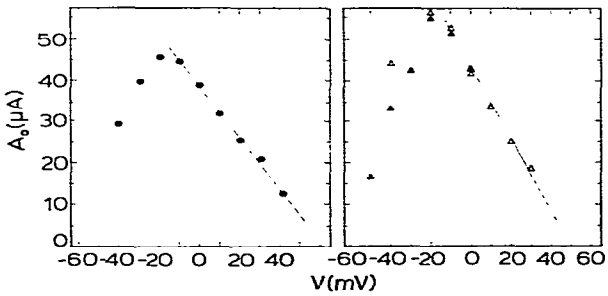

Fig. 9. The values of A_o in μA found from the least-squares fitting procedure plotted versus the absolute transmembrane potential. The values plotted on the left are calculated from the data of Kimura. The active area was 0.07 cm^2; the slope of the line is equivalent to a conductivity of 9.5×10^{-3} (Ω cm^2)$^{-1}$. The values plotted on the right are from the data of Meves in H_2O (▲) and ^2H_2O (△) on the same nerve. The straight line has a slope of 3.3×10^{-3} (Ω cm^2)$^{-1}$) for an area 0.25 cm^2. Other conditions of the experiments are listed in table 3.

Table 3

Experimental conditions and data for fig. 9

	Left (from Kimura)	Right (from Meves: solid points H_2O, open points ^2H_2O)
External media (mM)	460 Na^+	70 Na^+
Internal media	CsF	tetraethylammonium$^+$
Clamped area (cm^2)	0.07	0.25
Resting potential (mV)	−100	−78 (^2H_2O), −80 (H_2O)
Temperature (°C)	1.5	4
Slope of line (Ω cm^2)	106	300
Conductivity ($g_{Na} \cdot a_o$) (mmho cm^{-2})	9.6	3.3

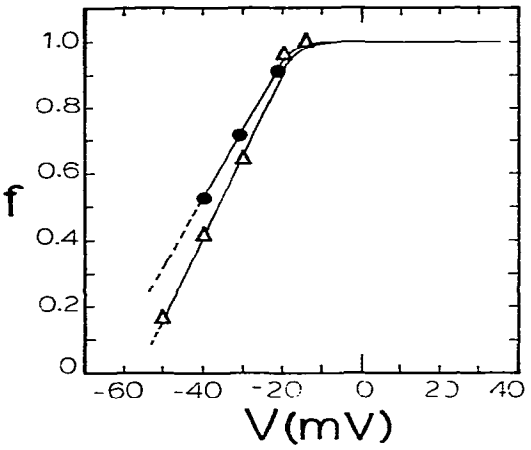

Fig. 10. Plot of the value of f, the fraction of channels open, versus the absolute transmembrane potential. (●) From Kimura's data, (△) from Meves data. As discussed in the text, this could be a fractional channel conductivity instead.

slope is due to the changing electrochemical potential, we extrapolate the line to more negative potentials to find the 'expected' current value in that region. However, these values are not reached in the experiments. Mindful of the arguments made in the beginning of this section concerning the meaning of f, we can assume that this behavior results entirely from having less than the total number of the channels being activated; f is less than 1. The values of f, the fraction of channels open, can then be calculated. These are displayed in fig. 10. Both nerves show quite similar behavior even though the holding potentials differed by 20 mV. The value of f seems to change linearly with the transmembrane potential before becoming constant near −10 mV absolute transmembrane potential. This is in excellent agreement with the results of Begenisich and Busath [29] as recently found in single-channel behavior. They interpreted this as being due to saturable Na^+ permeability.

From this limited sample, the properties of A_o appear to depend on the transmembrane potential and not on the potential jump size as do the kinetic parameters, σ, Δt and k_1. This difference in behavior partly explains the necessary complexity of models that have described the voltage-clamp results with absolute-voltage-dependent parameters only.

Possible tests for the various phenomena observed here might be to substitute different ions in the solutions such as done by Tasaki et al. [37] and fitting the data as done here. (To the author's knowledge, papers describing such voltage-clamp experiments report only changes in peak currents.)

To test whether the value of f is an indication of the channel number or channel conductivity, one might change the internal and external Na^+ concentrations simultaneously such as to hold the Nernst potential constant and see whether there is a change in the behavior of f. This might show up as a change in the voltage at which 'saturation' occurs: where the value of f becomes unity.

3.8. The present model and 'gating currents'

A number of experiments have been run attempting to find the 'gating currents' that accompany the kinetic processes responsible for the changes in Na^+ and K^+ conductances. This area of study has recently been reviewed by Almers [38] who clearly states the positive and negative evidence. The question reduces to whether the currents that are seen, generally called 'asymmetry currents', are related to the movement of charges in the membrane which result in the opening of

the Na^+ channel. As Almers points out, any charge motion observed will be inside the membrane. However, the origin of the 'leaky capacitive' currents is still obscure. Recently, Armstrong and Gilly [39] have detected numerous components in the asymmetry currents. They have put forth a model which in some aspects is similar to the author's [11]. While there are many possible correlations between the asymmetry currents and the channel opening, there is a strong argument for the disassociation of the two phenomena. At the suggestion of the author, Meves [15] showed that the asymmetry currents were unaffected by the use of ^2H_2O in place of H_2O. But the rates describing the Na^+ currents were changed markedly by the substitution. These results were confirmed by Schauf and Bullock [40]. On the other hand, there is the possibility that at least part of the asymmetry currents can be due to the surface charges responsible for the electric field shielding reflected in the Δt-process.

If the nerve is correctly described by the model presented here we, can state a conclusion with assurance about only one of the processes associated with the Na^+ currents. Since the slow turnoff upon prolonged depolarization, the k_2-process, is voltage independent, no voltage-dependent asymmetry currents are expected to be seen arising from it.

From the simple time course of the two, voltage-dependent processes, $(\Delta t, \sigma)$ and (k_1, β_m), it follows that the kinetics of the gating currents should follow closely. More important, changes with temperature, with changes of solvent, and with pulse protocol should be the same in order to claim that the gating currents could be related.

In contrast to the time course correlation, the magnitudes of the currents are open to wide surmise. This is so because of the wide range of reasonable presumptions that can be made about possible distances moved by the approx. 10 charges (for σ, Δt) or charges of unknown size (for k_1, β_m) over unknown fractions of the total potential. In addition, there is complete ambiguity concerning the number of sites. For instance, will the $(\Delta t, \sigma)$- or (k_1, β_m)-processes be characteristic of the whole membrane (one site/30 $Å^2$), of the number of transmembrane proteins (about 100-times the Na^+-current-blocking-toxin binding sites), or of the number of tetrodotoxin-saxitoxin binding sites ($\approx 100/\mu m^2 =$ one site/10^6 $Å^2$)? Additionally, we do not yet know if one toxin site comprises one 'channel'.

Because of the lack of any data illuminating answers to the above ambiguities, we must retract to the position that the gating currents must be found to follow the time course of the rates of the elemental processes. The currents that do not are most likely to be 'noise' from other (far more numerous and massive) parts of the membrane. The differences in the effect of ^2H_2O on the Na^+ currents and the gating currents supports the likelihood of such an origin.

Acknowledgments

I wish to thank Anthony Stone for help with the mathematical intricacies, Jack Lewis and P.F. Baker for encouragement and support, and Peter McNaughton and Frank Meeks for useful discussions. Part of this work was done while the author was in receipt of postdoctoral fellowships from the NIH-PHS, from NATO administered through the NSF, and from the SRC of England.

Appendix

A.1. Mathematical derivation of the current equation

The integrated form of the amount of 'C' in the reaction $A \xrightarrow{k_1} C \xrightarrow{k_2} D$ is given by

$$[C] = \frac{k_1}{k_2 - k_1}[A_o](e^{-k_1 t} - e^{-k_2 t}) \tag{A1}$$

when all the material is in the 'A' form initially, i.e., A_o. To this we convolute a Gaussian distribution of the form

$$P = (1/\sigma\sqrt{2\pi}) \exp(-u^2/2\sigma^2). \tag{A2}$$

For ease of computation, let $(1/\sigma\sqrt{2\pi}) = N$ and $[k_1/(k_2 - k_1)] = M$. For the time 'u' at which the pulse starts for the unconvoluted central point,

$$f_i(t, u) = \begin{cases} \exp[-k_i(t-u)] & t > u \\ 0 & t < u \end{cases}$$

The convolution of eqs. A1 and A2 is then

$$\int_{-\infty}^{\infty}[f_1(t,u)+f_2(t,u)]\,M\cdot N\cdot\exp(-u^2/2\sigma^2)\,du$$
$$= M\cdot N\int_{-\infty}^{t}[e^{-k_1(t-u)}-e^{-k_2(t-u)}]\,e^{-u^2/2\sigma^2}\,du$$
$$+ M\cdot N\int_{t}^{\infty}0\cdot e^{-u_2/2\sigma^2}\,du.$$

The actual start of the pulse will be a time Δt before the time u. The practical form of this equation can be derived by completing the squares. Each exponential is of the form

$$\exp\left[-(u^2/2\sigma^2)-k_i t-k_i u\right]$$
$$=\exp\left[-(u-k_i\sigma^2)^2/2\sigma^2-k_i t+\tfrac{1}{2}k_i^2\sigma^2\right]$$
$$=\exp(-k_i t+\tfrac{1}{2}k_i^2\sigma^2)\cdot\exp\left[-(u-k_i\sigma^2)^2/2\sigma^2\right]\,du$$

Reverting to our integral, there are two of the form

$$\exp(-k_i t+\tfrac{1}{2}k_i^2\sigma^2)\,NM\int_{-\infty}^{t}\exp\left[-(u-k_i\sigma^2)^2/2\sigma^2\right]\,du \tag{A3}$$

Let $S_i=\dfrac{u-k_i\sigma^2}{\sigma\sqrt{2}}$, then $dS_i=\dfrac{du}{\sigma\sqrt{2}}$.

When $u=t$, $S_i=\dfrac{1}{\sqrt{2}}(t/\sigma-k_i\sigma)$. However, the integral $(2/\sqrt{\pi})\int_{-\infty}^{t}\exp(-S^2)\,dS$ is the complementary error function, erfc(t). Thus, eq. A3 becomes

$$\exp(-k_i t+\tfrac{1}{2}k_i^2\sigma^2)\int_{\infty}^{\sqrt{2}^{-1}(t/\sigma-k_i\sigma)}\pi^{-1/2}\exp(-S^2)\,dS$$

where the integral equals $\frac{1}{2}$erfc.

$$I(t)=(2\sqrt{2}\sigma)^{-1}[A_0][k_1/(k_2-k_1)]$$
$$\times\left[\exp(-k_1 t+\tfrac{1}{2}k_1^2\sigma^2)\,\mathrm{erfc}(S_1)\right.$$
$$\left.-\exp(-k_2 t+\tfrac{1}{2}k_2^2\sigma^2)\,\mathrm{erfc}(S_2)\right] \tag{A4}$$

For the computer fit, the curve is calculated by convolution and then merely shifted in time Δt until the best fit is obtained. Thus, we substitute $t=(t-\Delta t)$ into eq. A4 to obtain the equation used with the computer program. That is

$$I(t)=(2\sqrt{2}\sigma)^{-1}[A_0][k_1/(k_2-k_1)]$$
$$\times\left\{\exp\left[-k_1(t-\Delta t)+\tfrac{1}{2}k_1^2\sigma^2\right]\cdot\mathrm{erfc}(S_1)\right.$$
$$\left.-\exp\left[k_2(t-\Delta t)+\tfrac{1}{2}k_2^2\sigma^2\right]\cdot\mathrm{erfc}(S_2)\right\} \tag{A5}$$

where erfc(S_i) uses $S_i=2^{-1/2}[(t-\Delta t)/\sigma-k_i\sigma]$.

References

1 A.L. Hodgkin, A.F. Huxley and B. Katz, J. Physiol. 116 (1952) 424.
2 A.L. Hodgkin and A.F. Huxley, J. Physiol. 116 (1952) 449.
3 A.L. Hodgkin and A.F. Huxley, J. Physiol. 116 (1952) 473.
4 A.L. Hodgkin and A.F. Huxley, J. Physiol. 117 (1952) 500.
5 A.C. Scott, Rev. Mod. Phys. 47 (1975) 487.
6 L.B. Cohen, Physiol. Rev. 53 (1973) 373.
7 J.W. Woodbury, S.H. White, M.C. Mackey, W.L. Hardy and D.B. Chang, in Physical chemistry, an advanced treatise, vol. 9B, ed. H. Eyring (Academic Press, New York, 1970) ch. 11.
8 G. Roy, Prog. Biophys. Mol. Biol. 29 (1975) 47.
9 C.P. Smyth, Dielectric behavior and structure (McGraw-Hill, New York, 1955) ch. 2.
10 K.S. Cole and R.H. Cole, J. Chem. Phys. 9 (1941) 341.
11 K.A. Rubinson, J. Physiol. 281 (1978) 14P.
12 K.A. Rubinson, Biophys. Chem. 12 (1980) 51.
13 H. Meves, Prog. Biophys. Mol. Biol. 33 (1978) 207.
14 W.K. Chandler and H. Meves, J. Physiol. 180 (1965) 788.
15 H. Meves, J. Physiol. 243 (1974) 847.
16 a. R. Huber, Nature 280 (1979) 538 and references therein; b. M. Karplus and J.A. McCammon, CRC Crit. Rev. Biochem. 11 (1981) 293 and references therein.
17 J. Skolnick and E. Helfand, J. Chem. Phys. 72 (1980) 5489.
18 M.A. DeSando, S. Walker and W.H. Baarschers, J. Chem. Phys. 73 (1980) 3460.
19 L. Tronstad and K. Stokland, Det. K. Nor. Vidensk. Selsk. 10 (1938) 141.
20 J.T. Davies and E.K. Rideal, Interfacial phenomena (Academic Press, New York, 1963) ch. 2.
21 R.B. Dean, O. Gatty and E.K. Rideal, Trans. Faraday Soc. 36 (1940) 161.
22 R.A. Robinson and R.H. Stokes, Electrolyte solutions, 2nd edn., (Butterworths, London, 1959) ch. 2.
23 W. Jost, Diffusion in solids, liquids, gases (Acadmic Press, New York, 1960).
24 M. Schindler, D.E. Koppel and M.P. Sheetz, Proc. Natl. Acad. Sci. U.S.A. 77 (1980) 1457.
25 R. Horn, J. Patlak and C.F. Stevens, Nature 291 (1981) 426.
26 B.R. Ware and W.H. Flygare, Chem. Phys. Lett. 12 (1971) 81.
27 J. Albery, Electrode kinetics (Clarendon Press, Oxford, 1975) ch. 1.
28 R. Andubert, Disc. Faraday Soc. 1 (1947) 72.
29 T. Begenisich and D. Busath, J. Gen. Physiol. 77 (1981) 489.
30 D. D'Aprano and R.M. Fuoss, J. Phys. Chem. 73 (1969) 223.
31 L. Onsager, Phys. Rev. 54 (1938) 554.
32 A. Mozumder, J. Chem. Phys. 60 (1974) 4300.
33 J.L. Metzger and H. Labhart, Chem. Phys. 11 (1975) 441.
34 G.R. Freeman, J. Chem. Phys. 39 (1963) 1580.
35 R.R. Chance and C.L. Braun, J. Chem. Phys. 64 (1976) 3573.
36 G.S. Oxford and J.P. Pooler, J. Gen. Physiol. 66 (1975) 765.
37 I. Tasaki, I. Singer and A. Watanabe, Am. J. Physiol. 211 (1960) 746.

38 W. Almers, Rev. Physiol. Biochem. Pharmacol. 82 (1978) 96.
39 C.M. Armstrong and W.F. Gilly, J. Gen. Physiol. 74 (1979) 691.
40 C.L. Schauf and J.O. Bullock, Biophys. J. 30 (1980) 295.